Anion-Controlled Nuclearity and Metal−Metal Distances in Copper(I)−dppm Complexes (dppm = Bis(diphenylphosphino)methane)

Jitendra K. Bera, Munirathnam Nethaji, and Ashoka G. Samuelson*

Department of Inorganic and Physical Chemistry, Indian Institute of Science, Bangalore 560 012, India

Received May 6, 1998

Dicapped triangular copper(I)−dppm complexes $Cu_3(dppm)_3(\mu_3\text{-}X)_2^+$ (X = Cl, Br, and I) and monocapped $Cu_3(dppm)_3(\mu_3\text{-}OH)^{2+}$ have been prepared by treating the dimeric $Cu_2(dppm)_2(CH_3CN)_4(ClO_4)_2$ or $Cu_2(dppm)_2(dmcn)_3(BF_4)_2$ (dmcn = dimethylcyanamide) complexes with the corresponding bridging ligand X^-. The trimeric complexes $Cu_3(dppm)_3(\mu_3\text{-}OH)(BF_4)_2$ and $Cu_3(dppm)_3(\mu_3\text{-}Cl)_2Cl$ can be converted to dimers $Cu_2(dppm)_2(dmcn)_3(BF_4)_2$ and $Cu_2(dppm)_2(dmcn)(Cl)_2$ by reaction with HBF_4, dmcn, and excess dmcn, respectively. The complexes synthesized by the above means, $Cu_3(dppm)_3(\mu_3\text{-}Cl)_2ClO_4$ (**1**), $Cu_3(dppm)_3(\mu_3\text{-}Br)_2ClO_4$ (**2**)·2THF, $Cu_3(dppm)_3(\mu_3\text{-}I)_2I\cdot 2CH_2Cl_2\cdot CH_3OH$ (**3**), and $Cu_2(dppm)_2(dmcn)(Cl)_2\cdot 2dmcn$ (**4**) have been characterized by IR, ^1H and $^{31}P\{^1H\}$ NMR, and solid-state emission spectroscopy. The solid-state molecular structures of complexes **2**, **3**, and **4** were determined from single-crystal X-ray diffraction studies. Apart from confirming the nuclearity, the structural information reveals interesting variations in the Cu···Cu distances in dimeric and trimeric complexes. A simple geometric correlation between the Cu−X and Cu···Cu distances is noted in the trimeric complexes with an important exception of the dicapped Cl complex. Ab initio electronic structure calculations of the homo dicapped $Cu_3X_2^+$ (X= Cl, Br, HO, and HC_2) and mixed-capped Cu_3XY^+ (X = Cl, Y = HC_2) species have been carried out at the MP2 level of theory using valence-DZP-quality basis sets with effective core potentials on copper. The computed Cu···Cu distances reproduce the observed experimental trend. Analyses of the electronic structures of the optimized model $Cu_3X_2^+$ complexes reveal the electronic tuning of Cu···Cu distances by the capping ligand. The variation of Cu···Cu distances in monobridged dimeric copper(I)−dppm complexes can also be rationalized along similar lines.

Introduction

Bis(diphenylphosphino)methane (dppm) forms polynuclear complexes with most metal ions.[1] Among these is a ubiquitous series, $M_3(dppm)_3$, formed by late transition metal ions.[2] Interestingly when M is Cu(I), a capping ligand invariably accompanies the $Cu_3(dppm)_3$ core.[3] Monocapped and dicapped μ_3-bridged complexes are known. In the absence of a suitable cap, a dimeric complex is usually formed.[4] Another feature of interest in these trimeric systems is the variation in the M···M distances. In the case of late transition metal ions, M−M interactions are usually repulsive due to the nearly filled or fully filled d-shell of electrons. The closed-shell interactions between the d^{10} metal centers have been analyzed by Pyykkö.[5] This repulsive interaction is mitigated by relativistic contraction in the case of 5d metal ions such as Au(I). As a result, several polynuclear gold complexes with short Au−Au distances are well-known.[6] An estimate of aurophilic (Au−Au) interactions is also available from experimental and theoretical calcula-

(1) (a) Morton, D. A. V.; Orpen, A. G. *J. Chem. Soc., Dalton Trans.* **1992**, 641, and references therein. (b) Chaudret, B.; Delavaux, B.; Poilblanc, R. *Coord. Chem. Rev.* **1988**, *86*, 191. (c) Puddephatt, R. J. *Chem. Soc. Rev.* **1983**, *12*, 99.

(2) (a) Xiao, J.; Hao, L.; Puddephatt, R. J.; Manojlovic-Muir, L.; Muir, K. W. *J. Am. Chem. Soc.* **1995**, *117*, 6316. (b) Hao, L.; Xiao, J.; Vittal, J. J.; Puddephatt, R. J. *Angew. Chem., Int. Ed. Engl.* **1995**, *34*, 346. (c) Maekawa, M.; Munakata, M.; Kuroda-Sowa, T.; Hachiya, K. *Inorg. Chim. Acta* **1995**, *233*, 1. (d) Xiao, J.; Kristof, E.; Vittal, J. J.; Puddephatt, R. J. *J. Organomet. Chem.* **1995,** *490*, 1. (e) Xiao, J.; Puddephatt, R. J. Manojlovic-Muir, L.; Muir, K. W. *J. Am. Chem. Soc.* **1994**, *116*, 1129. (f) Rashidi, M.; Kristof, E.; Vittal, J. J.; Puddephatt, R. J. *Inorg. Chem.* **1994**, *33*, 1497. (g) Mirza, H. A.; Vittal, J, J.; Puddephatt, R. J. *Inorg. Chem.* **1993**, *32*, 1327. (h) Lloyd, B. R.; Manojlovic-Muir, L.; Muir, K. W.; Puddephatt, R. J. *Organometallics* **1993**, *12*, 1231. (i) Xiao, J.; Vittal, J. J.; Puddephatt, R. J.; Manojlovic-Muir, L.; Muir, K. W. *J. Am. Chem. Soc.* **1993**, *115*, 7882. (j) Manojlovic-Muir, L.; Muir, K. W.; Mirza, H. A.; Puddephatt, R. J. *Organometallics* **1992**, *11*, 3440. (k) Jennings, M. C.; Puddephatt, R. J.; Manojlovic-Muir, L.; Muir, K. W.; Mwariri, B. N. *Organometallics* **1992**, *11*, 4164. (l) Puddephatt, R. J.; Manojlovic-Muir, L.; Muir, K. W. *Polyhedron* **1990,** *9*, 2767. (m) Franzoni, D.; Pelizzi, G.; Predieri, G.; Tarasconi, P.; Vitali, F.; Pelizzi, C. *J. Chem. Soc., Dalton Trans.* **1989**, 247. (n) Hämmerle, B.; Müller, E. P.; Wilkinson, D. L.; Müller, G.; Peringer, P. *J. Chem. Soc., Chem. Commun*. **1989**, 1527. (o) Manojlovic-Muir, L.; Muir, K. W.; Lloyd, B. R.; Puddephatt, R. J. *J. Chem. Soc., Chem. Commun*. **1983**, 1336. See also ref 28a for a triangulo $Hg_2Ag(dppm)_3^{3+}$ cluster.

(3) (a) Diez, J.; Gamasa, M. P.; Gimeno, J.; Aguirre, A.; García-Granda, S. *Organometallics* **1997**, *16*, 3684. (b) Diez, J.; Gamasa, M. P.; Gimeno, J. *Polyhedron* **1995,** *14*, 741. (c) Chan, C.-K.; Guo, C.-X.; Wang, R.-J.; Mak, Thomas C. W.; Che C.-M. *J. Chem. Soc., Dalton Trans.* **1995**, 753. (d) Cuesta, R.; Ruiz, J.; Moreno, J. M.; Colacio, E. *Inorg. Chim. Acta* **1994**, *227*, 43, and the references in Table 7.

(4) (a) Harvey, P. D.; Drouin, M.; Zhang, T. *Inorg. Chem.* **1997**, *36*, 4998. (b) Ruina, Y.; Kunhua, L.; Yimin, H.; Dongmei, W.; Douman, J. *Polyhedron* **1997,** *16*, 4033. (c) Lanfredi, A. M. M.; Ugozzoli, F.; Camus, A.; Marsich, N.; Capelletti, R. *Inorg. Chim. Acta* **1993,** *206*, 173. (d) Lanfredi, A. M. M.; Ugozzoli, F.; Camus, A.; Marsich, N. *Inorg. Chim. Acta* **1985,** *99*, 111. For more examples on $Cu_2(dppm)_2$ complexes, also see refs 15, 16, and 48.

(5) Pyykkö, P. *Chem. Rev.* **1997**, *97*, 597.

(6) (a) Mingos, D. M. P.; Yau, J.; Menzer, S.; Williams, D. J. *J. Chem. Soc., Dalton Trans* **1995**, 319. (b) Davila, R. M.; Elduque, A.; Grant, T.; Staples, R. J.; Fackler, J. P. *Inorg. Chem.* **1993**, *32*, 1749. (c) Schmidbaur, H. *Gold Bull*. **1990**, *23*, 11. (d) Balch, A. L.; Fung, E. Y.; Olmstead, M. M. *J. Am. Chem. Soc.* **1990**, *112*, 5181. (e) King, C.; Wang, J.-C.; Khan, N. I. Md.; Fackler, J. P. *Inorg. Chem.* **1989**, *28*, 2185. (f) Schmidbaur, H.; Graf, W.; Müller, G. *Angew. Chem., Int. Ed. Engl*. **1988**, *27*, 417. (g) Khan, N. I. Md.; Wang, S.; Heinrich, D. D.; Fackler, J. P. *Acta Crystallogr*. **1988**, *C44*, 822.

10.1021/ic980515f CCC: $18.00
Published on Web 12/30/1998

tions.[5,7] However, the existence of analogous metallophilic effects in the case of Cu(I) has been the subject of a long debate.[8] Recently, two examples of complexes[9,10] having unsupported short Cu(I)−Cu(I) contacts have come to light, and the possibility of *cuprophilicity* has been noted. However, the presence of such attractive interactions in these cases has been refuted by DFT calculations recently.[11] In copper complexes then, the M−M distances are primarily dictated by the ligand or by electrostatic forces. In the systems under consideration, the bite size of the dppm ligand is a determining factor. However, the wide variation in the Cu···Cu distances observed in $Cu_3(dppm)_3$ complexes suggests an important role for the capping ligand. The average Cu···Cu distances are 2.570(3) Å in dicapped acetylide complex[12] and 3.322(2) Å in the monocapped hydroxo complex.[13] By structural characterization of a series of complexes with different caps, it should be possible to examine the role of the caps in orchestrating the trinuclear core and fine-tuning the Cu···Cu distances.

In this study, an efficient synthetic route to prepare the trinuclear Cu(I)−dppm complexes of the general formulas $[Cu_3(dppm)_3(\mu_3\text{-}X)_2]^+$ (X = Cl, Br, I, and HO) is presented starting from dinuclear $Cu_2(dppm)_2$ complexes. Through reactivity studies on the interconversion of these trinuclear and dinuclear complexes, the role of the cap in organizing a trinuclear core is brought out. Ab initio electronic structure calculations are performed on model complexes to help one understand the role of bridging ligands in controlling the Cu···Cu distances in polynuclear complexes.

Experimental Section

Instruments and Measurements. ^{1}H NMR spectra were recorded with a Bruker ACF 200 MHz spectrometer operating at 81.1 MHz, and $^{31}P\{^1H\}$ NMR spectra on a Bruker AMX 400 MHz spectrometer operating at 162 MHz. Chemical shifts were calibrated to tetramethylsilane and 85% H_3PO_4 as external references for ^{1}H and $^{31}P\{^1H\}$ NMR, respectively. All the ^{1}H and $^{31}P\{^1H\}$ NMR spectra were recorded in $CDCl_3$ solution. Infrared spectra were measured on a Bio-Rad FTS-7 spectrophotometer. Elemental analyses were done with a Carlo Erba Elemental Analyzer 1106. Emission spectra were recorded on a Hitachi F-2000 spectrophotometer. Freshly prepared crystals of the complexes were used for the emission study.

Materials and Methods. Dichloromethane, petroleum ether (bp 60−80 °C), tetrahydrofuran, and acetonitrile were purified and dried by conventional methods, distilled under nitrogen, and deoxygenated before use. Methanol was distilled and used as such. $[Cu(CH_3CN)_4]BF_4$ and $[Cu(CH_3CN)_4]ClO_4$ were freshly prepared before use. (*Caution! Perchlorate salts of metal complexes with organic ligands are potentially explosive. While we have faced no untoward incident in their preparation and studies, it is preferable that only small amounts are prepared at a time and handled with great caution.*) Bis(diphenylphosphino)methane and tetrabutylammonium bromide were purchased from Aldrich. Dimethylcyanamide was bought from Fluka. CuCl[14] and complexes $Cu_2(dppm)_2(dmcn)_3(BF_4)_2$,[15] $Cu_2(dppm)_2(CH_3CN)_4(ClO_4)_2$,[16] and $Cu_3(dppm)_3(\mu_3\text{-}Cl)_2Cl$[17] have been synthesized following the literature procedure. All other chemicals were obtained from Ranbaxy (India). All reactions were carried out in an atmosphere of dried N_2 using standard Schlenk and vacuum line techniques.

Synthesis of $Cu_3(dppm)_3(\mu_3\text{-}Cl)_2ClO_4$ (1). The complex $Cu_2(dppm)_2(CH_3CN)_4(ClO_4)_2$ (0.205 g, 0.16 mmol) and sodium chloride (0.150 g, 2.57 mmol) were stirred in 1:2 CH_2Cl_2/THF (30 mL) for 8 h. The reaction mixture was filtered, and the solvent was removed under vacuum. The solid residue was redissolved in CH_2Cl_2 and filtered, and the colorless filtrate was concentrated to dryness under reduced pressure. Trituration with the addition of petroleum ether resulted in the formation of **1**, which was filtered, washed with petroleum ether (3 × 5 mL), and dried under vacuum. Analytically pure material was obtained by recrystallization from a mixture of CH_2Cl_2 and petroleum ether (yield 72%). Anal. Found (calcd) for $Cu_3P_6Cl_3C_{75}H_{66}O_4$: C 59.08 (59.49), H 4.36 (4.40). ^{1}H NMR: δ 3.20 (6 H, m, CH_2 protons of dppm); 6.80−7.16 (60 H, m, C_6H_5 protons of dppm). $^{31}P\{^1H\}$: δ −14.73 (s). IR data (cm^{-1}): dppm 3057(w), 1579(w), 1481(m), 1430(m), 771(w), 740(m), 695(s), 516(m), 475(m); ClO_4^- 1093(vs, br), 621(m).

Synthesis of $Cu_3(dppm)_3(\mu_3\text{-}Br)_2ClO_4$ (2). Tetrabutylammonium bromide (0.068 g, 0.21 mmol) was added to a CH_2Cl_2 solution (20 mL) of $Cu_2(dppm)_2(CH_3CN)_4(ClO_4)_2$ (0.180 g, 0.14 mmol) and stirred for 2 h. The solvent was removed under reduced pressure, and the white residue was washed with petroleum ether. It was redissolved in 1:1 CH_2Cl_2/CH_3OH (5 mL), layered with petroleum ether, and kept at 4 °C. White crystals of **2** separated out from the solution after 20 days (yield 38%). Anal. Found (calcd) for $Cu_3P_6Br_2C_{75}H_{66}ClO_4$: C 56.31 (56.19), H 4.11 (4.16). ^{1}H NMR: δ 3.25 (6 H, m, CH_2 protons of dppm); 6.91−7.14 (60 H, m, C_6H_5 protons of dppm). $^{31}P\{^1H\}$: δ −17.36 (s), −16.05 (w). IR data (cm^{-1}): dppm 3051(w), 1484(m), 1430(m), 771(w), 736(m), 695(s), 513(m), 479(m); ClO_4^- 1091(vs, br), 622(m).

Synthesis of $Cu_3(dppm)_3(\mu_3\text{-}Br)_2ClO_4$ (2)·2THF. Bromobenzene (0.03 mL, 0.28 mmol) was allowed to react with Li metal (0.030 g) in dry THF (30 mL) for 2 h. A solution of $Cu_2(dppm)_2(CH_3CN)_4(ClO_4)_2$ (0.186 g, 0.15 mmol) in THF (5 mL) was added to the reaction mixture and stirred for 1 h and filtered, and the solvent was removed under vacuum. The solid residue was redissolved in CH_2Cl_2 and filtered, and the colorless filtrate was concentrated to dryness under reduced pressure. Trituration with the addition of petroleum ether resulted in the formation of a white solid, which was washed with petroleum ether (3 × 5 mL). Crystals were obtained by layering the THF solution of the complex with petroleum ether (yield 62%). Anal. Found (calcd) for $Cu_3P_6Br_2C_{83}H_{82}ClO_6$: C 56.82 (57.05), H 4.71 (4.74). The spectroscopic data are identical to those described earlier for $Cu_3(dppm)_3(\mu_3\text{-}Br)_2ClO_4$ (**2**) with additional peaks due to the solvent of crystallization, THF, in the ^{1}H NMR spectrum.

Synthesis of $Cu_3(dppm)_3(\mu_3\text{-}I)_2I\cdot 2CH_2Cl_2\cdot CH_3OH$ (3). The complex $Cu_2(dppm)_2(CH_3CN)_4(ClO_4)_2$ (0.180 g, 0.14 mmol) and potassium iodide (0.150 g, 0.90 mmol) were stirred in 1:2 CH_2Cl_2/CH_3OH (30 mL) for 2 h. The reaction mixture was filtered, and the colorless filtrate was concentrated to dryness under reduced pressure. Trituration with the addition of petroleum ether resulted in the formation of a white solid, which was washed with petroleum ether (3 × 5 mL). Crystals were obtained by layering the CH_2Cl_2 solution of the complex with petroleum ether (yield 66%). ^{1}H NMR: δ 3.37 (6 H, m, CH_2 protons of dppm); 6.91−7.17 (60 H, m, C_6H_5 protons of dppm). $^{31}P\{^1H\}$: δ −22.48 (s). IR data (cm^{-1}): dppm 3053(w), 1482(m), 1430(m), 771(w), 736(m), 695(s), 513(m), 479(m).

Synthesis of $Cu_3(dppm)_3(\mu_3\text{-}OH)(BF_4)_2$ from $Cu_2(dppm)_2(dmcn)_3(BF_4)_2$. The complex $Cu_3(dppm)_3(OH)(BF_4)_2$ was prepared using a

(7) (a) Harwell, D. E.; Mortimer, M. D.; Knobler, C. B.; Anet, F. A. L.; Hawthorne, M. F. *J. Am. Chem. Soc.* **1996**, *118*, 2679. (b) Narayanaswamy, R.; Young, M. A.; Parkhurst, E.; Ouellette, M.; Kerr, M. E.; Ho, D. M.; Elder, R. C.; Bruce, A. E.; Bruce, M. R. M. *Inorg. Chem.* **1993**, *32*, 2506. (c) Dziwok, K.; Lachmann, J.; Wilkinson, D. L.; Müller, G.; Schmidbaur, H. *Chem. Ber.* **1990**, *123*, 893. (d) Schmidbaur, H.; Dziwok, K.; Grohmann, A.; Müller, G. *Chem. Ber.* **1989**, *122*, 893.

(8) Abraham, S. P.; Samuelson, A. G.; Chandrasekhar, J. *Inorg. Chem.* **1993**, *32*, 6107, and references therein.

(9) Singh, K.; Long, J. R.; Stavropoulos, P. *J. Am. Chem. Soc.* **1997**, *119*, 2942.

(10) Siemeling, U.; Vorfeld, U.; Neumann, B.; Stammler, H.-G. *Chem. Commun.* **1997**, 1723.

(11) Poblet, J.-M.; Bénard, M. *Chem. Commun.* **1998**, 1179.

(12) Diez, J.; Gamasa, M. P.; Gimeno, J.; Lastra, E.; Aguirre, A.; García-Granda, S. *Organometallics* **1993**, *12*, 2213.

(13) Ho, D.; Bau, R. *Inorg. Chem.* **1983**, *22*, 4079.

(14) Keller, R. N.; Wycoff, H. D. *Inorganic Syntheses*; Vol. 2, p 1.

(15) Bera, J. K.; Nethaji, M.; Samuelson, A. G. Submitted for publication.

(16) Diez, J.; Gamasa, M. P.; Gimeno, J.; Tiripicchio, A.; Camellini, M. T. *J. Chem. Soc., Dalton Trans.* **1987**, 1275.

(17) Marsich, N.; Camus, A.; Cebulec, E. *J. Inorg. Nucl. Chem.* **1972,** *34*, 933.

Table 1. Crystallographic Data for $Cu_3(dppm)_3(\mu_3\text{-}Br)_2ClO_4$ (**2**)·2THF, $Cu_3(dppm)_3(\mu_3\text{-}I)_2I\cdot 2CH_2Cl_2\cdot CH_3OH$ (**3**), and $Cu_2(dppm)_2(dmcn)(Cl)_2\cdot 2dmcn$ (**4**)

	compound		
	2·2THF	**3**	**4**
empirical formula	$C_{83}H_{66}Br_2ClCu_3O_6P_6$	$C_{78}H_{66}Cl_4Cu_3I_3OP_6$	$C_{59}H_{62}Cl_2Cu_2N_6P_4$
fw	1731.07	1918.25	1177.01
crystal system	monoclinic	orthorhombic	monoclinic
temp (K)	293	293	293
λ (Å)	0.7107	0.7107	0.7107
space group	$P2_1$	$Pbn2_1$	$P2_1/n$
a (Å)	10.773(3)	18.983(3)	13.457(5)
b (Å)	26.760(3)	19.823(3)	24.230(4)
c (Å)	14.557(4)	20.551(4)	17.803(5)
α (deg)			
β (deg)	101.25(3)		90.91(3)
γ (deg)			
V (Å^3)	4116(2)	7734(2)	5804(3)
Z	2	4	4
ρ_{calcd} (g/cm^3)	1.397	1.648	1.347
abs coeff (cm^{-1})	19.37	23.21	9.78
F(000)	1752	3784	2440
no. of ind reflns	7392	8655	10 176
no. of data/restraints/params	7392/29/328	8646/1/325	10146/0/674
final R1,[a] wR2[b] [$I > 2\sigma(I)$]	0.0869, 0.2152	0.0845, 0.2078	0.0563, 0.1374
final R1,[a] wR2[b] (all data)	0.1542, 0.2361	0.1382, 0.2567	0.0763, 0.1675
GOF[c]	1.037	1.127	1.047

[a] $R1 = (\sum||F_o| - |F_c||)/(\sum|F_o|)$. [b] $wR2 = [\sum w(|F_o|^2 - |F_c|^2)^2/\sum w|F_o|^2)^2]^{1/2}$. [c] $GOF = [w(F_0^2 - F_c^2)^2]/(n - p)^{1/2}$.

modified procedure slightly different from that of Bau et al.[13] A solution of $Cu_2(dppm)_2(dmcn)_3(BF_4)_2$ (0.110 g, 0.09 mmol) in CH_2Cl_2 (5 mL) was stirred in hot methanol for 4 h. A white precipitate started appearing on reducing the volume of the reaction mixture. It was filtered, washed with cold methanol (3 × 5 mL), and dried under vacuum. Crystals were obtained from a mixture of CH_2Cl_2 and petroleum ether (yield 57%).^{1}H NMR: δ 3.21 (6 H, m, CH_2 protons of dppm); 6.81−7.14 (60 H, m, C_6H_5 protons of dppm). $^{31}P\{^1H\}$: δ −15.26 (s).

Conversion of $Cu_3(dppm)_3(\mu_3\text{-}OH)(BF_4)_2$ to $Cu_2(dppm)_2(dmcn)_3(BF_4)_2$. A solution of $Cu_3(dppm)_3(\mu_3\text{-}OH)(BF_4)_2$ (0.130 g; 0.08 mmol), HBF_4 (0.05 mL), and dmcn (0.10 mL, 1.23 mmol) in CH_2Cl_2 was stirred for 2 h at room temperature. Removal of solvent under reduced pressure resulted in an oily residue. Addition of petroleum ether gave a white precipitate, which was filtered and washed with the same solvent (3 × 5 mL). Crystals were obtained by layering petroleum ether on a CH_2Cl_2 solution of $Cu_2(dppm)_2(dmcn)_3(BF_4)_2$ (yield 91%).^{1}H NMR: δ 2.92 (18 H, CH_3 protons of dmcn); 3.55 (6 H, m, CH_2 protons of dppm); 7.12−7.27 (60 H, m, C_6H_5 protons of dppm). $^{31}P\{^1H\}$: δ −9.98 (s).

Conversion of $Cu_3(dppm)_3(\mu_3\text{-}Cl)_2Cl$ to $Cu_2(dppm)_2(dmcn)(Cl)_2\cdot 2dmcn$ (4). A solution of $Cu_3(dppm)_3(\mu_3\text{-}Cl)_2(Cl)$ (0.150 g, 0.10 mmol) in CH_2Cl_2 (20 mL) was treated with an excess of dmcn (1 mL) and stirred for 30 min. The volume of the resulting solution was reduced under reduced pressure. The concentrated solution was then transferred to a Schlenk tube and kept at 4 °C. White crystals of **4** separated out after 7−10 days. The crystals were thoroughly washed with petroleum ether and dried under vacuum (yield 71%). Anal. Found (calcd) for $Cu_2P_4C_{59}H_{62}N_6Cl_2$: C 60.05 (60.20), 5.40 (5.32); N 7.31 (7.14). ^{1}H NMR: δ 2.85 (18 H, CH_3 protons of dmcn); 3.22 (4 H, m, CH_2 protons of dppm); 6.91−7.14 (40 H, m, C_6H_5 protons of dppm). $^{31}P\{^1H\}$: δ −15.24 (s). IR data (cm^{-1}): dppm 3053(w), 1482(m), 1430(m), 771(w), 736(m), 695(s), 513(m), 479(m); dmcn 2217.

X-ray Data Collection, Structure Solution, and Refinement

General. Crystals of **2** and **4,** suitable for diffraction studies, were glued to the tip of glass fibers and transferred to a computer-controlled Enraf-Nonius CAD4 diffractometer with graphite-monochromatized Mo Kα radiation. The crystals of **3** rapidly become opaque outside the solvent of crystallization. Hence, they were mounted in a Lindemann capillary along with the mother liquor. Accurate unit cell parameters and orientation matrixes were determined by least-squares refinement of 25 well-centered reflections in the range $10° \le \theta \le 18°$. Three periodically measured reference reflections showed no significant decay (<5%) during the time of data collection. Crystal data and the relevant experimental details on data collection and refinement for **2**, **3**, and **4** are collected in Table 1. Data collected at 20 °C were corrected for Lorentz and polarization effects. The position of the heavy atoms were determined by Patterson methods using SHELXS86.[18] The remaining atoms were found from difference Fourier analyses using SHELXL-93.[19] An empirical absorption correction was applied to the data of all the crystals.[20]

$Cu_3(dppm)_3(\mu_3\text{-}Br)_2ClO_4$ (2)·2THF. A colorless rectangular crystal suitable for diffraction study was used for the data collection. A total of 8140 reflections were collected in the range $1.43° \le \theta \le 24.97°$. The carbon atoms of phenyl rings of the dppm ligands were located from difference Fourier maps and refined as rigid groups. Only copper, bromine, and phosphorus atoms were refined anisotropically. During the course of the structure refinement, two molecules of THF were found cocrystallized with the complex in the asymmetric unit. Atoms of the THF molecules and the ClO_4^- anion were located and subsequently refined with restraint. The hydrogen atoms of the dppm ligands were included in the final stage of the refinement on calculated positions bonded on their carrier atoms. The highest peak remaining in the final difference map was 1.012 e Å^{-3} and located in the vicinity of one of the disordered THF molecules. The final R value obtained was 0.087.

$Cu_3(dppm)_3(\mu_3\text{-}I)_2I\cdot 2CH_2Cl_2\cdot CH_3OH$ (3). A suitable single crystal was sealed in a Lindemann capillary along with the mother liquor and used for data collection. Intensity data of 9237 reflections were collected in the range $1.46° \le \theta \le 26.97°$. The carbon atoms of the phenyl rings of the dppm ligands were located from the difference Fourier maps and refined as rigid groups. During the course of the structure refinement, two molecules of CH_2Cl_2 and one molecule of CH_3OH were found cocrystallized with the complex. Atoms of these solvent molecules were located and refined satisfactorily. Only copper, phosphorus, and iodine atoms were refined anisotropically. Hydrogen atoms were included in the final stage of the refinement on calculated positions bonded on their carrier atoms. The highest remaining peak

(18) Sheldrick, G. M. *SHELXS*-86: Program for Crystal Structure Determination; University of Cambridge: Cambridge, England, 1986.
(19) Sheldrick, G. M. *SHELXL-93*: A Program for Crystal Structure Refinement; University of Göttingen: Germany, 1993.
(20) Parkin, S.; Moezzi, B.; Hope, H. *J. Appl. Crystallogr.* **1995**, *28*, 53.

in the final difference Fourier was 1.41 e Å^{-3} and located in the vicinity of the Cu_3I_2 core. The final R value obtained was 0.084.

$Cu_2(dppm)_2(dmcn)(Cl)_2$·2dmcn (4). A colorless needle-shaped crystal was washed with petroleum ether to remove the dmcn ligand adhering to the surface. Intensity data of 11 016 reflections were collected in the range $1.42° \leq \theta \leq 24.97°$. The structure was found to contain two molecules of isolated dmcn molecules in the asymmetric unit. All non-hydrogen atoms were refined with anisotropic thermal parameters except the methyl carbons of the dmcn ligands. Hydrogen atoms were included in the final stage of the refinement on calculated positions bonded on their carrier atoms. The highest peak in the final difference map of 1.042 e Å^{-3} was located at a distance of 0.93 Å from Cu1. Convergence was reached at $R = 0.056$.

Theoretical Methods and Systems Studied

Ab initio calculations with relatively large basis sets, including electron correlation, have been carried out using well-tested theoretical procedures.[21] For the metal, effective core potentials (ECPs) proposed by Hay and Wadt[22] were employed. As recommended by Frenking and co-workers,[21e] only the 1s, 2s, and 2p orbitals on copper are treated as the core. The contraction scheme corresponding to HW3DZ2P(441/2111/41), in the notation of these authors, was employed.[23] The ligand atoms were described using the 6-31G(d) basis set.[24] Structures of all the species considered in this study were optimized at the MP2 level[25] using the Gaussian-94[26] suite of programs. The final wave functions were subsequently subjected to a natural population (NPA) and bond orbital (NBO) analysis.[27]

Ab initio study on the real inorganic complexes is difficult due to the relatively large basis sets required for the metal and the huge ligand systems. As the dppm ligand is common to all the complexes studied in this paper, we have excluded it in the model. Calculations have been carried out on homo dicapped $Cu_3X_2^+$ where X is Cl, Br, HO, and HC_2 and the mixed ligand $Cu_3Cl(C_2H)^+$ cores. The geometry of the homo and mixed dicapped systems are idealized to D_{3h} and C_{3v} symmetry, respectively. The lowest energy closed-shell singlet state has been considered for all the species.

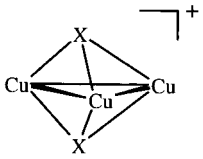

X = Cl^-, Br^-, HO^-, HC_2^-

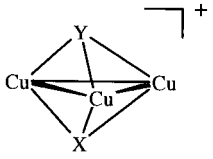

X = Cl^-, Y = HC_2^-

Results

Solid-State Molecular Structures. X-ray crystal structures of **2**, **3**, and **4** were determined to confirm the nuclearity and to obtain the Cu···Cu distances in these complexes. The molecular structures of complexes **2** and **3** are similar, and we discuss it together.

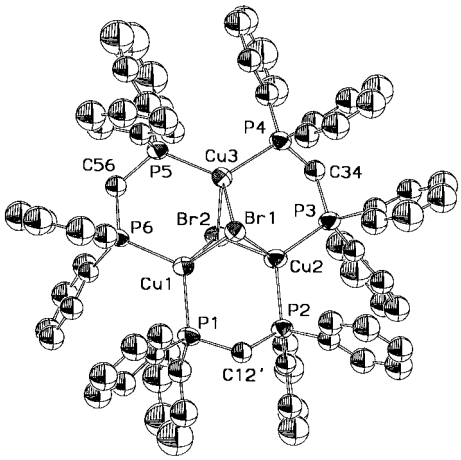

Figure 1. X-ray structure of the $Cu_3(dppm)_3(\mu_3\text{-}Br)_2^+$ unit in the crystal of **2**·THF. Hydrogen atoms are omitted for clarity.

Solid-State Structure of $Cu_3(dppm)_3(\mu_3\text{-}Br)_2ClO_4$ (2)·2THF and $Cu_3(dppm)_3(\mu_3\text{-}I)_2I$·$2CH_2Cl_2$·$CH_3OH$ (3). The solid-state structures of both **2** and **3** consist of a cationic $Cu_3(dppm)_3(\mu_3\text{-}X)_2^+$ (X = Br, I) core. The three copper atoms form a triangle with a dppm ligand bridging each edge to form a Cu_3P_6 core. The dicapping halide ions are bonded to the three copper atoms in a μ_3 fashion from opposite faces of the triangle. The Cu_2P_2C rings adopt envelope conformations with the methylene carbon atoms on the flap, one of them folded toward one of the faces, and the other two away from it. This two-up-one-down conformation is found in analogous trimeric $M_3(dppm)_3$ clusters.[2] The disposition of the phenyl rings of the dppm ligand is interesting in both complexes. The two phenyl rings attached to a phosphorus center stay on opposite sides of the plane formed by the three copper centers. Therefore, the $M_3(dppm)_3$ core creates two hydrophobic cavities consisting of six phenyl rings. Several "noncoordinating" anions can be trapped inside this cavity. Others[28] and we[29] have recently structurally characterized complexes with oxyanions ($CF_3SO_3^-$, WO_4^{2-}) inside this cavity.

The crystal structure of **2** consists of a trinuclear $Cu_3(dppm)_3(\mu_3\text{-}Br)_2^+$ and a discrete ClO_4^- anion. The structure together with the selected atomic numbering scheme is depicted in Figure 1. Important bond distances and bond angles are given in Table 2. The copper atoms are tetracoordinate, each being bonded to

(21) (a) Bera, J. K.; Samuelson, A. G.; Chandrasekhar, J. *Organometallics* **1998**, *17*, 4136. (b) Frenking, G.; Pidun, U. *J. Chem. Soc., Dalton Trans.* **1997**, 1653. (c) Neuhaus, A.; Veldkamp, A.; Frenking, G. *Inorg. Chem.* **1994**, *33*, 5278. (d) Böhme, M.; Frenking, G.; Reetz, M. T. *Organometallics* **1994**, *13*, 4237. (e) Ehlers, A. W.; Frenking, G. *J. Am. Chem. Soc.* **1994**, *116*, 1514. (f) Jonas, V.; Frenking, G.; Reetz, M. T. *Organometallics* **1993**, *12*, 2111. (g) Cundari, T. R.; Gordon, M. S. *Organometallics* **1992**, *11*, 55.

(22) Hay, P. J.; Wadt, W. R. *J. Chem. Phys.* **1985**, *82*, 299.

(23) Jonas, V.; Frenking, G.; Reetz, M. T. *J. Comput. Chem.* **1992**, *13*, 919.

(24) The basis sets used for H, C, O, and Cl atoms were provided with the *Gaussian-94* program. The basis set for Br has been taken from: Binning, R. C.; Curtiss, L. A. *J. Comput. Chem.* **1990**, *11*, 1206.

(25) (a) Binkley, J. S.; Pople, J. A. *Int. J. Quantum Chem.* **1975**, *9*, 229. (b) Møller, C.; Plesset, M. S. *Phys. Rev.* **1934**, *46*, 618.

(26) Frisch, M. J.; Trucks, G. W.; Schlegel, H. B.; Gill, P. M. W.; Johnson, B. G.; Robb, M. A.; Cheeseman, J. R.; Keith, T.; Petersson G. A., Montgomery, J. A.; Raghavachari, K.; Al-Laham, M. A.; Zakrzewski, V. G.; Ortiz, J. V.; Foresman, J. B.; Cioslowski, J.; Stefanov, B. B.; Nanayakkara, A.; Challacombe, M.; Peng, C. Y.; Ayala, P. Y.; Chen, W.; Wong, M. W.; Andres, J. L.; Replogle, E. S.; Gomperts, R.; Martin, R. L.; Fox, D. J.; Binkley, J. S.; Defrees, D. J.; Baker, J.; Stewart, J. P.; Head-Gordon, M.; Gonzalez, C.; Pople, J. A. *Gaussian 94, Revision C.2*; Gaussian, Inc.: Pittsburgh, PA, 1995.

(27) (a) Reed, A. E.; Curtis, L. A.; Weinhold, F. *Chem. Rev.* **1988**, *88*, 899. (b) Reed, A. E.; Weinhold, F. *J. Am. Chem. Soc.* **1986**, *108*, 3586. (c) Reed, A. E.; Weinstock, R. B.; Weinhold, F. *J. Chem. Phys.* **1985**, *83*, 735. (d) Reed, A. E.; Winhold, F. *J. Chem. Phys.* **1985**, *83*, 1736.

(28) (a) Knoepfler, A.; Wurst, K.; Peringer, P. *J. Chem. Soc., Chem. Commun.* **1995**, 131. In a recent publication, Harvey et al. have shown that even an elusive anion PF_6^- can be trapped inside the cavity generated by the $Pd_3(dpam)_3$ core, where dpam ($Ph_2As-CH_2-AsPh_2$) is an arsenic analogue of dppm: Zhang, P.; Drouin, M.; Harvey, P. D. *Chem. Commun.* **1996,** 877. In the solid-state structure of $Cu_3(dppm)_3(\mu_3\text{-}OH)(BF_4)_2$ (ref 13), two BF_4^- anions are situated in the hydrophobic cavities above and below the Cu_3 triangle.

(29) Recently we have structurally established a trinuclear complex $Cu_3(dppm)_3(\mu_3\text{-}Cl)(\mu_3,\eta^1\text{-}OWO_3)$ (ref 15). The WO_4^{2-} stays inside the cavity through coordination of an oxygen to the copper atoms and the weak hydrogen bonding interactions between oxygen atoms of the oxyanion and hydrogen atoms of the phenyl and methylene groups of the dppm ligands.

two bromine and two phosphorus atoms. The Cu−P bond distances vary over a small range of 2.241(5)−2.259(4) Å, which appear significantly longer than those found in the complex $(CuBr)_2$dppm (mean 2.19(1) Å).[30] The two bromine atoms are nearly equidistant from the plane formed by the three copper atoms (1.898 and 1.909 Å, respectively, for Br1 and Br2). Br1 binds the copper atoms with one long (2.676(2) Å) and two short (2.545(3) and 2.583(3) Å) bonds, whereas Br2 binds the copper atoms with one short (2.575 (2) Å) and two long (2.628(3) and 2.629(3) Å) bonds. A similar arrangement was observed for the dicapped Cl complex.[31] The Cu···Cu separation in this complex (3.005(3)−3.128(3) Å) is significantly shorter than that found in the analogous dicapped chloro[31] or the monocapped hydroxo complex.[13]

The crystal structure of **3** consists of a trinuclear $Cu_3(dppm)_3(\mu_3\text{-}I)_2^+$ and an isolated I^- anion. The structure together with the selected atomic numbering scheme is depicted in Figure 2. Important bond distances and bond angles are given in Table 3. The copper atoms are tetracoordinate, each being bonded to two iodine and two phosphorus atoms. The Cu−P distances vary from 2.226(9) to 2.269(11) Å. Two iodine atoms (I1 and I2) are at a distance 2.054 and 2.061 Å from the plane formed by the three copper atoms, respectively. A related complex $Cu_3(dppm)_2(\mu_2\text{-}I)(\mu_3\text{-}I)_2$ has been known for a long time.[32] In complex **3**, the μ_2-bridged iodide is replaced by a dppm ligand. The mean Cu···Cu distance (3.165(5) Å) is longer than in the dicapped Br (3.081(3) Å) complex **2** but marginally shorter than in the Cl analogue (3.210(4) Å).

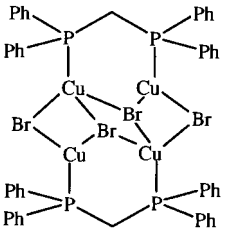

$[(CuBr)_2(dppm)]_2$

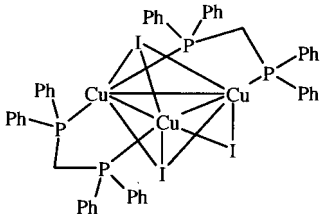

$[Cu_3(dppm)_2I_3]$

Solid-State Molecular Structure of $Cu_2(dppm)_2(dmcn)(Cl)_2\cdot 2dmcn$ (4). The solid-state structure of this complex can be described as a neutral $[Cu_2(dppm)_2(\mu_2\text{-}Cl)(\eta^1\text{-}Cl)(\eta^1\text{-}dmcn)]$ species. The structure together with the selected atomic numbering scheme is depicted in Figure 3. Important bond distances and bond angles are given in Table 4. In this dimeric complex, two copper atoms are doubly bridged by two dppm ligands to form an eight-member $Cu_2P_4C_2$ ring. Atoms Cu1 and Cu2 are terminally bonded to a nitrogen atom (N1) of dmcn ligand and

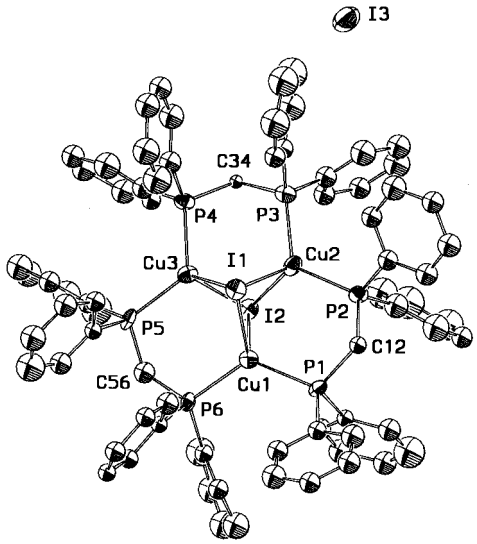

Figure 2. X-ray structure of the $Cu_3(dppm)_3(\mu_3\text{-}I)_2I$ unit in the crystal of **3**. Hydrogen atoms are omitted for clarity.

Table 2. Selected Bond Distances (Å) and Angles (deg) of $Cu_3(dppm)_3(\mu_3\text{-}Br)_2ClO_4$ (**2**)·2THF

Bond Distances			
Cu(1)−Cu(2)	3.005(3)	Cu(3)−P(5)	2.241(5)
Cu(1)−Cu(3)	3.128(3)	Cu(3)−P(4)	2.258(5)
Cu(2)−Cu(3)	3.110(3)	Cu(3)−Br(2)	2.575(2)
Cu(1)−P(6)	2.247(5)	Cu(3)−Br(1)	2.676(2)
Cu(1)−P(1)	2.247(4)	P(1)−C(12′)	1.86(2)
Cu(1)−Br(1)	2.545(3)	P(2)−C(12′)	1.81(2)
Cu(1)−Br(2)	2.628(3)	P(3)−C(34)	1.84(2)
Cu(2)−P(3)	2.247(5)	P(4)−C(34)	1.82(2)
Cu(2)−P(2)	2.259(4)	P(5)−C(56)	1.85(2)
Cu(2)−Br(1)	2.583(3)	P(6)−C(56)	1.82(2)
Cu(2)−Br(2)	2.629(3)		

Bond Angles			
Cu(1)−Cu(2)−Cu(3)	61.51(7)	P(5)−Cu(3)−Br(2)	105.1(2)
Cu(2)−Cu(3)−Cu(1)	57.58(6)	P(4)−Cu(3)−Br(2)	106.5(2)
Cu(2)−Cu(1)−Cu(3)	60.91(8)	P(5)−Cu(3)−Br(1)	110.7(1)
P(6)−Cu(1)−P(1)	118.4(2)	P(4)−Cu(3)−Br(1)	111.0(2)
P(6)−Cu(1)−Br(1)	117.2(2)	Br(1)−Cu(1)−Br(2)	94.83(9)
P(1)−Cu(1)−Br(1)	108.3(2)	Br(1)−Cu(2)−Br(2)	93.92(9)
P(6)−Cu(1)−Br(2)	100.3(1)	Br(2)−Cu(3)−Br(1)	92.99(7)
P(1)−Cu(1)−Br(2)	115.3(2)	Cu(1)−Br(1)−Cu(2)	71.72(7)
P(3)−Cu(2)−P(2)	120.7(2)	Cu(1)−Br(1)−Cu(3)	73.56(7)
P(3)−Cu(2)−Br(1)	118.4(2)	Cu(2)−Br(1)−Cu(3)	72.49(7)
P(2)−Cu(2)−Br(1)	105.4(1)	Cu(3)−Br(2)−Cu(1)	73.90(8)
P(3)−Cu(2)−Br(2)	100.3(2)	Cu(3)−Br(2)−Cu(2)	73.39(8)
P(2)−Cu(2)−Br(2)	115.2(2)	Cu(1)−Br(2)−Cu(2)	69.70(6)
P(5)−Cu(3)−P(4)	125.2(2)		

Cl2, respectively, in addition to the two phosphorus atoms of two different dppm ligands. The tetrahedral geometry of copper atoms is satisfied by a bridging Cl ligand. The Cu1−Cl1 (2.348(1) Å) and Cu2−Cl1 (2.488(2) Å) distances are significantly different. Cu2 forms a shorter bond with the terminally bonded Cl2 (2.362(2) Å). The coordination asymmetry of the copper centers is reflected in the copper−phosphorus distances. The Cu1−P1 and Cu1−P2 are shorter than the Cu2−P3 and Cu2−P4 distances.

The distorted tetrahedral environment around the metal centers is also reflected in the angles reported in Table 4. The P1−Cu1−P2 angle is larger than the ideal tetrahedral value of 109°. Surprisingly, the Cu1−N1−C12 angle deviates from 180°. The Cu1−Cl1−Cu2 bridging angle is acute, suggesting 3c-2e electron deficient bridging. It has the most acute bridge angle among the monobridged dimeric $Cu_2(dppm)_2$ complexes.[33] The

(30) Camus, A.; Nardin, G.; Randaccio, L. *Inorg. Chim. Acta* **1975**, *12*, 23.
(31) Bresciani, N.; Marsich, N.; Nardin, G.; Randaccio, L. *Inorg. Chim. Acta* **1974**, *10*, L5.
(32) Nardin, G.; Randaccio, L.; Zangrando, E. *J. Chem. Soc., Dalton Trans.* **1975**, 2566.

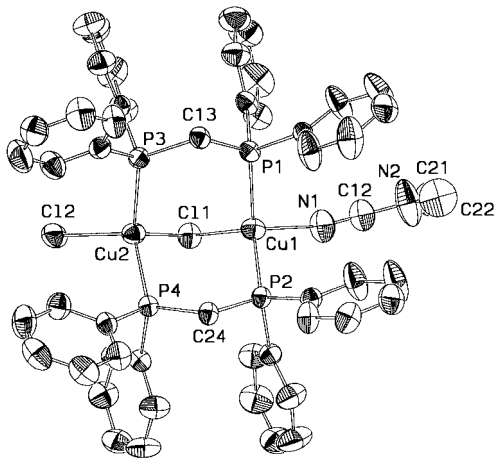

Figure 3. X-ray structure of the $Cu_2(dppm)_2(dmcn)(Cl)_2$ unit in the crystal of **4**. Hydrogen atoms are omitted for clarity.

Table 3. Selected Bond Distances (Å) and Angles (deg) of $Cu_3(dppm)_3(\mu_3\text{-}I)_2I\cdot 2CH_2Cl_2\cdot CH_3OH$ (**3**)

Bond Distances			
Cu(1)−Cu(2)	3.111(3)	Cu(3)−P(5)	2.249(10)
Cu(1)−Cu(3)	3.184(5)	Cu(3)−P(4)	2.252(9)
Cu(2)−Cu(3)	3.199(6)	Cu(3)−I(1)	2.754(2)
Cu(1)−P(6)	2.257(10)	Cu(3)−I(2)	2.755(2)
Cu(1)−P(1)	2.309(9)	P(1)−C(12)	1.89(3)
Cu(1)−I(1)	2.727(5)	P(2)−C(12)	1.78(3)
Cu(1)−I(2)	2.765(5)	P(3)−C(34)	1.85(2)
Cu(2)−P(2)	2.226(9)	P(4)−C(34)	1.89(2)
Cu(2)−P(3)	2.269(11)	P(5)−C(56)	1.72(3)
Cu(2)−I(2)	2.744(5)	P(6)−C(56)	1.83(3)
Cu(2)−I(1)	2.766(5)		

Bond Angles			
Cu(1)−Cu(2)−Cu(3)	60.6(2)	P(5)−Cu(3)−I(1)	113.6(3)
Cu(1)−Cu(3)−Cu(2)	58.34(6)	P(4)−Cu(3)−I(1)	112.3(3)
Cu(2)−Cu(1)−Cu(3)	61.1(2)	P(5)−Cu(3)−I(2)	104.1(3)
P(6)−Cu(1)−P(1)	123.7(4)	P(4)−Cu(3)−I(2)	103.8(3)
P(6)−Cu(1)−I(1)	113.6(3)	I(1)−Cu(1)−I(2)	97.1(2)
P(1)−Cu(1)−I(1)	106.0(3)	I(1)−Cu(3)−I(2)	96.65(6)
P(6)−Cu(1)−I(2)	100.8(3)	I(2)−Cu(2)−I(1)	96.6(2)
P(1)−Cu(1)−I(2)	112.4(3)	Cu(1)−I(1)−Cu(3)	71.02(13)
P(2)−Cu(2)−P(3)	120.7(4)	Cu(1)−I(1)−Cu(2)	68.99(6)
P(2)−Cu(2)−I(2)	115.0(3)	Cu(2)−I(2)−Cu(3)	71.14(13)
P(3)−Cu(2)−I(2)	101.7(3)	Cu(2)−I(2)−Cu(1)	68.76(6)
P(2)−Cu(2)−I(1)	106.7(3)	Cu(3)−I(1)−Cu(2)	70.83(13)
P(3)−Cu(2)−I(1)	113.6(3)	Cu(3)−I(2)−Cu(1)	70.45(13)
P(5)−Cu(3)−P(4)	122.0(2)		

eight-member $Cu_2P_4C_2$ ring adopts the more common *boat* conformation.[34]

Emission Spectra. The solid-state emission spectra of complexes **1**−**4**, dimeric complexes $Cu_2(dppm)_2(dmcn)_3(BF_4)_2$ and $Cu_2(dppm)_2(CH_3CN)_4(ClO_4)_2$, and the trimeric $Cu_3(dppm)_3(OH)(BF_4)_2$ were measured at room temperature. The emission and excitation maxima have been tabulated in Table 5. Representative spectra are given in Figure 4. The emission maxima of the dimeric $Cu_2(dppm)_2(CH_3CN)_4(ClO_4)_2$ and $Cu_2(dppm)_2(dmcn)_3(BF_4)_2$ complexes are centered around 482 and 470 nm, respectively. Complex **1** shows a very broad band with the emission maxima around 511 nm. However, the emission spectra of complexes **2** and **3** exhibit multiple bands. Irradiation of complex **2** around 340 nm gives a weak band at 484 nm and two broad overlapping bands with their maxima around 514 and 566 nm. Complex **3**, too, exhibits multiple emission bands at 466, 520, and 574 nm on irradiation around 335 nm. The emission spectrum of complex **4** is similar to that of other dinuclear $Cu_2(dppm)_2$ complexes.[15]

Table 4. Selected Bond Distances (Å) and Angles (deg) of $Cu_2(dppm)_2(dmcn)(Cl)_2\cdot 2dmcn$ (**4**)[a]

Bond Distances			
Cu(1)−Cu(2)#1	3.293(1)	Cu(2)−Cl(2)#2	2.362(2)
Cu(1)−P(1)	2.258(1)	Cu(2)−Cl(1)#1	2.488(2)
Cu(1)−P(2)	2.248(1)	P(1)−C(13)	1.830(4)
Cu(1)−N(1)	2.158(5)	P(2)−C(24)	1.833(4)
Cu(1)−Cl(1)	2.348(1)	P(3)−C(13)	1.848(4)
Cu(2)−P(3)#1	2.265(1)	P(4)−C(24)	1.845(4)
Cu(2)−P(4)#1	2.273(1)		

Bond Angles			
Cu(1)−Cl(1)−Cu(2)#1	85.80(5)	N(1)−C(12)−N(2)	177.6(6)
N(1)−Cu(1)−P(2)	102.70(14)	P(3)#1−Cu(2)−P(4)#1	125.50(5)
N(1)−Cu(1)−P(1)	99.51(14)	P(3)#1−Cu(2)−Cl(2)#2	104.75(5)
P(2)−Cu(1)−P(1)	125.09(5)	P(4)#1−Cu(2)−Cl(2)#2	109.17(5)
N(1)−Cu(1)−Cl(1)	109.51(12)	P(3)#1−Cu(2)−Cl(1)#1	107.92(5)
P(2)−Cu(1)−Cl(1)	112.28(5)	P(4)#1−Cu(2)−Cl(1)#1	104.04(5)
P(1)−Cu(1)−Cl(1)	106.22(5)	Cl(2)#2−Cu(2)−Cl(1)#1	103.53(5)
C(12)−N(1)−Cu(1)	154.2(4)		

[a] Symmetry transformations used to generate equivalent atoms: #1 = $-x, -y+1, -z+1$. #2 = $-x+1/2, y+1/2, -z+1/2$.

Table 5. Solid-State Emission and the Corresponding Excitation Maxima[a] of Complexes **1**−**4**, $Cu_2(dppm)_2(dmcn)_3(BF_4)_2$, $Cu_2(dppm)_2(CH_3CN)_4(ClO_4)_2$, and $Cu_3(dppm)_3((oh)(BF_4)_2$

no.	complex	λ_{max}^{em} (nm)	λ_{max}^{ex} (nm)
1	$Cu_2(dppm)_2(dmcn)_3(BF_4)_2$	470	366
2	$Cu_2(dppm)_2(CH_3CN)_4(ClO_4)_2$	482	357
3	$Cu_2(dppm)_2(dmcn)(Cl)_2\cdot 2dmcn$ (**4**)	480	374
4	$Cu_3(dppm)_3(\mu_3\text{-}OH)(BF_4)_2$[b]	510	356
5	$Cu_3(dppm)_3(\mu_3\text{-}Cl)_2ClO_4$ (**1**)	511	381
6	$Cu_3(dppm)_3(\mu_3\text{-}Br)_2ClO_4$ (**2**)·2THF	484, 514, 566	344, 373
7	$Cu_3(dppm)_3(\mu_3\text{-}I)_2I\cdot 2CH_2Cl_2\cdot CH_3OH$ (**3**)	466, 520, 574	333, 366

[a] See text for details. [b] Values are similar to that reported in ref 45.

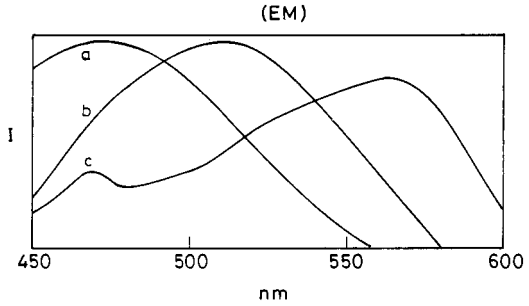

Figure 4. Solid-state emission spectra of $Cu_2(dppm)_2(dmcn)_3(BF_4)_2$ (a), complex **1** (b), and **3** (c) recorded at room temperature.

Discussion

Synthesis and the Changes in Nuclearity. The copper(I)−dppm complexes containing the triangular $Cu_3(dppm)_3$ framework supported by two capping ligands can be prepared starting from the dimeric complexes, $Cu_2(dppm)_2(dmcn)_3(BF_4)_2$ or Cu_2-

(33) The Cu−X−Cu angles in monobridged $Cu_2(dppm)_2(\mu_2\text{-}dmcn)(dmcn)_2(BF_4)_2$ (**6b**) and $Cu_2(dppm)_2(\mu_2\text{-}OClO_3)(dmcn)_2(ClO_4)$ (**6d**) complexes (Figure 6) are 90.9(2)° and 94.8(2)°, respectively. The corresponding angle in complex **4** is 85.80(5)°.

(34) In most of $Cu_2(dppm)_2$ complexes, the $Cu_2P_4C_2$ ring adopts a *boat* conformation. A few examples are $Cu_2(dppm)_2(NO_3)_2$ (**6a**), $Cu_2(dppm)_2(dmcn)_3(BF_4)_2$ (**6b**), $Cu_2(dppm)_2(CH_3COO)(BF_4)$ (ref 4a), etc. However, the complex $Cu_2(dppm)_2(dmcn)_2(\mu_2\text{-}OClO_3)(ClO_4)$ (**6d**) adopts a *chair* conformation. The weak hydrogen bonding interaction between an oxygen atom of μ_2-$OClO_3$ and one of the methylene protons stabilizes this conformation (ref 15).

$(dppm)_2(CH_3CN)_4(ClO_4)_2$. On treatment with halide anions X^- (X = Cl, Br, or I), they readily convert to trimeric species of the general formulas $Cu_3(dppm)_3(\mu_3\text{-}X)_2^+$. The triangular Cu(I)−dppm complex with chloride capping ligands has been synthesized[17] earlier by the reaction of CuCl with dppm and structurally characterized.[31] Recently, preparation of the identical cationic moiety has been carried out by reacting the dimeric $Cu_2(dppm)_2(AcO)BF_4$ with Me_3SiCl.[3b] We have prepared the complex $Cu_3(dppm)_3(\mu_3\text{-}Cl)_2ClO_4$ (**1**) by treating the $Cu_2(dppm)_2(CH_3CN)_4(ClO_4)_2$ with NaCl in CH_2Cl_2/THF (1:1) solution.

The analogous Br complex $Cu_3(dppm)_3(\mu_3\text{-}Br)_2ClO_4$ (**2**) has been prepared by the addition of tetrabutylammonium bromide to the dimeric $Cu_2(dppm)_2(CH_3CN)_4(ClO_4)_2$. The solid-state structure has also been confirmed by an X-ray diffraction study.[35] A complex containing the identical core was obtained in an attempt to make a $Cu_3(dppm)_3$ complex with $C_6H_5^-$ as capping ligands. The dimer $Cu_2(dppm)_2(CH_3CN)_4(ClO_4)_2$ was treated with $C_6H_5^-$ prepared from C_6H_5Br and Li in THF. The isolated complex corresponded to $Cu_3(dppm)_3(\mu_3\text{-}Br)_2ClO_4 \cdot 2THF$ (**2**·2THF). A single-crystal X-ray diffraction study confirmed the trinuclear structure and the noninvolvement of two molecules of THF in the lattice.

The trinuclear Cu(I) complex containing only two dppm units and both capping and edge-bridged iodide ligands has been structurally characterized previously.[32] To make a meaningful comparison of the Cu···Cu bond distances in $Cu_3(dppm)_3(\mu_3\text{-}X)_2^+$ with various halide anions, it was necessary to prepare an analogous iodo complex. This was obtained by the treatment of $Cu_2(dppm)_2(CH_3CN)_4(ClO_4)_2$ (Cu:dppm is 1:1) with NaI. The structure of the cationic core $Cu_3(dppm)_3(\mu_3\text{-}I)_2^+$ is identical to that of trimeric Cl and Br derivatives. The only difference in complex **3** is that it contains I^- as a counteranion instead of the noncoordinated ClO_4^- present in **1** and **2**.

An attempt was made to prepare the dicapped fluoro complex by employing biphasic reaction conditions. An aqueous solution containing sodium fluoride and a CH_2Cl_2 solution of $Cu_2(dppm)_2(dmcn)_3(BF_4)_2$ were stirred together for 12 h. The isolated compound was invariably $Cu_3(dppm)_3(OH)(BF_4)_2$. Treatment of $Cu_2(dppm)_2(dmcn)_3(BF_4)_2$ with warm methanol also gives $Cu_3(dppm)_3(OH)(BF_4)_2$. We are aware of only three examples of structurally characterized monocapped $Cu_3(dppm)_3$ cores in the literature.[36] Treatment of $Cu_2(dppm)_2(dmcn)_3(BF_4)_2$ with NaOH in THF does not lead to a dicapped hydroxo species, but oxidation of the dppm ligand occurs.[37] Although the dicapped hydroxo complex has not been synthesized successfully to date, the trimeric copper(I)−dppm complex with phenolate anions as the capping ligands has been synthesized and structurally characterized recently.[38]

The trimeric $Cu_3(dppm)_3(OH)^{2+}$ on treatment with HBF_4 and dmcn converts to dimeric $Cu_2(dppm)_2(dmcn)_3(BF_4)_2$. This reaction occurs at room temperature and is complete in 30 min. The unavailability of one lone pair as in the protonation of the capping ligand of $Cu_3(dppm)_3(OH)(BF_4)_2$ results in the collapse of the trimeric structure. The conversion from a trimer to a dimer is not facile when the capping ligands are Cl^-. The $^{31}P\{^1H\}$ signal of $Cu_3(dppm)_3(\mu_3\text{-}Cl)_2Cl$ does not change on the addition

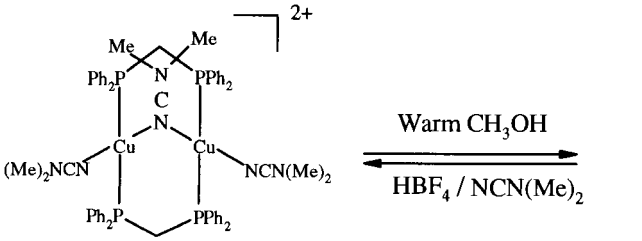

$[Cu_2(dppm)_2(dmcn)_3]^{2+}$

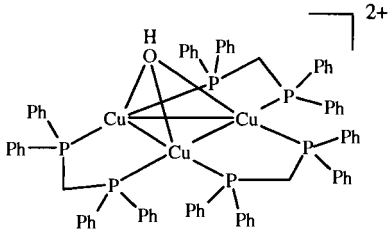

$[Cu_3(dppm)_3(OH)]^{2+}$

of excess dmcn. But treatment of $Cu_3(dppm)_3(\mu_3\text{-}Cl)_2Cl$ with excess dmcn and subsequent crystallization gives complex **4**. Although the dimeric nature of $Cu_2(dppm)_2(dmcn)(Cl)_2$ is confirmed by the single crystal study, the ^1H NMR and $^{31}P\{^1H\}$ NMR of **4** are indicative of trimeric species $Cu_3(dppm)_3(\mu_3\text{-}Cl)_2Cl$ in solution.[39] The presence of excess dmcn probably results in an equilibrium from which the dimeric species crystallizes out preferentially. In solution, the labile dmcn comes out of the coordination sphere and it forms a trimer.

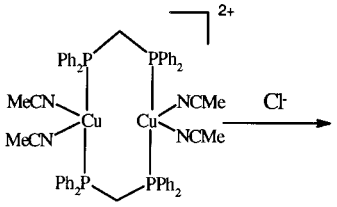

$[Cu_2(dppm)_2(MeCN)_4]^{2+}$

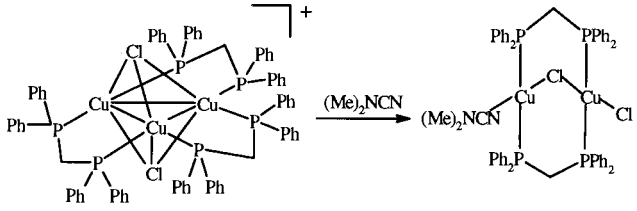

$[Cu_3(dppm)_3(Cl)_2]^+$ $[Cu_2(dppm)_2(Cl)_2(dmcn)]$

A survey of the recently reported Cu(I)−dppm dimeric complexes with various anions vide infra and Cu(I)−dppm trimeric complexes with different capping ligands (Table 6) clearly indicates that the nuclearity of these species is determined by the bridging ligand. The addition of halides (with the

(35) Crystal data for **2**: $Cu_3P_6Br_2C_{75}H_{66}ClO_4$, triclinic, space group $P1$, a = 15.208(2) Å, b = 17.904(2) Å, c = 26.915(4) Å, α = 97.123(3)°, β = 90.211(2)°, γ = 103.144(3)°, V = 7077.6(8) Å^3, Z = 4.

(36) Yam, Vivian W.-W.; Lee, W.-K.; Cheung, K.-K.; Crystall, B.; Phillips, D. *J. Chem. Soc., Dalton Trans.* **1996**, 3283. The other two examples are given in refs 12 and 13.

(37) Bera, J. K.; Samuelson, A. G. Unpublished results.

(38) Wycliff, C. Ph.D. Thesis, Indian Institute of Science, Bangalore, 1997.

(39) Consistently higher negative values in the ^{31}P NMR spectra are noted for trinuclear $Cu_3(dppm)_3$ complexes compared to the dinuclear $Cu_2(dppm)_2$ complexes. The values vary over a smaller range of −9.0 to −12.0 ppm in the case of dimers and −14.5 to −22.5 ppm in the case of trimers. One exception among dimers is complex **4**. Interestingly, acetylide as the capping ligand reduces the magnitude of ^{31}P NMR values of the trimers. In fact, the lowest value (−5.5 ppm) is obtained for the dicapped acetylide complex. For details, see ref 15.

Table 6. Cu···Cu and Cu−X/Y Distances (Å) in Triangular Monocapped $Cu_3(dppm)_3(\mu_3\text{-}X)^{2+}$ and Dicapped $Cu_3(dppm)_3(\mu_3\text{-}X)(\mu_3\text{-}Y)^+$ Complexes

complex		distance			
X	Y	Cu···Cu	Cu···Cu (average)	Cu−X/Y	ref
HO		3.120(2), 3.127(2), 3.322(2)	3.190(2)	1.996(6)−2.026(6)	13
Bu−C≡C		2.910(1), 2.941(2), 3.175(1)	3.009(1)	1.997(9)−2.067(8)	36
Ph−C≡C		2.813(2), 2.904(3), 3.274(3)	2.997(3)	1.96(1)−2.08(1)	12
Cl	Cl	3.175(4), 3.175(4), 3.281(3)	3.210(4)	2.407(7)−2.678(6)	31
I	I	3.111(3), 3.184(5), 3.199(6)	3.165(5)	2.727(5)−2.765(5)	*c*
Br	Br	3.005(3), 3.110(3), 3.128(3)	3.081(3)	2.545(3)−2.676(2)	*c*
Cl	OWO_3	3.032(5), 3.077(5), 3.090(5)	3.066(5)	2.16(2)−2.25(2)[a]	15
Me−C_6H_4−O	Me−C_6H_4−O	3.023(5), 3.030(5), 3.069(5)	3.041(5)	2.11(2)−2.30(2)	38
Cl	Ph−C≡C	2.803(3), 2.785(3), 2.871(3)	2.820(3)	1.98(2)−2.34(2)[b]	12
Ph−C≡C	Ph−C≡C	2.570(3), 2.598(3), 2.615(3)	2.594(3)	2.06(2)−2.34(2)	12

[a] Values given are for Cu−O distances. The range of Cu−Cl distances are 2.506(8)−2.563(8). [b] Values given are for Cu−C distances. [c] This work.

Table 7. Optimized Geometry and Selected NBO Analysis Data of $Cu_3(\mu_3\text{-}X)_2^+$ and $Cu_3(\mu_3\text{-}X)(\mu_3\text{-}Y)^+$ Systems at the MP2 Level of Theory

system		distance (Å)			WBI ($\times 10^3$)			occupancy	
X	Y	Cu···Cu	Cu−X	Cu−Y	Cu···Cu	Cu−X	Cu−Y	Cu (4s)	Cu (4p)
Cl	Cl	2.884	2.405	2.405	5	102	102	0.10	0.01
Br	Br	2.811	2.497	2.497	8	145	145	0.15	0.02
HO	HO[a]	2.763	2.047	2.047	6	87	87	0.08	0.02
Cl	H−C≡C[b]	2.649	2.441	2.100	11	102	127	0.12	0.02
H−C≡C	H−C≡C[c]	2.511	2.148	2.148	14	115	115	0.13	0.02

[a] Additional bond distances in Å: O−H = 0.973. [b] C−H = 1.075; C−C = 1.249. [c] C−H = 1.075; C−C = 1.249.

exception of F^-) leads to the ready formation of trimers, whereas the weakly coordinated oxyanions give dimers. From the series of complexes listed in Table 6, it is apparent that the formation of a trimer requires a ligand capable of donating one σ and two π lone pairs. Oxyanions, where the lone pairs are delocalized, form dimeric structures[4a−c,15] with the exception of $Cu_3(dppm)_3(\mu_3\text{-}Cl)(\mu_3\text{-}OWO_3)$.[15] In this case, the presence of Cl^- could be responsible for the formation of the trimeric species.

Metal−Metal Distances. As mentioned earlier, the Cu··· Cu distances in di- and polynuclear Cu(I)−dppm complexes should be primarily controlled by the bite size of the dppm ligand. In the series of complexes studied here, bridged by dppm and capping ligands, the caps play an important role in fine-tuning the metal−metal distances. Cu···Cu distances in a series of μ_3-bridged mono- and dicapped $Cu_3(dppm)_3$ complexes are given in Table 6. The range of Cu−X/Y distances where X and Y are the capping atoms has also been given in the table. In most cases the triangle formed by the three copper atoms is not equilateral, and hence the average Cu···Cu distance is listed for purposes of comparison.

The dicapped complexes have smaller Cu···Cu distances than the corresponding monocapped analogues. The average Cu···Cu distance in the diacetylide (2.594(3) Å) complex is significantly shorter than the monocapped acetylide complex (2.997(3) Å). Although no dihydroxo species has been structurally characterized, the dicapped phenoxo (−OC_6H_4−CH_3) complex[38] (3.041(5) Å) provides a suitable comparison and is shorter than that of the mono hydroxo complex (3.190(2) Å).[13]

Among dicapped halide complexes, there is an anomalous variation in the Cu···Cu distances. The observed distances are longest for the Cl complex and smallest for Br complex, and the I complex has a longer distance than the Br complex as expected! The values listed in Table 6 indicate a simple geometric correlation between Cu−X/Y and Cu···Cu distances among dicapped complexes with the exception of the Cl complex. In a Cu_3X_2 framework, longer Cu−X distances should lead to larger Cu···Cu separations purely due to geometrical constraints. This correlation seems to be valid in the case of the dicapped phenoxo complex too. The only exception is the dichloro complex, which has the shortest Cu−X distances among the halide series, but it has the longest Cu···Cu distances.

Cu···Cu distances in phenylacetylide-bridged complexes are significantly shorter. The average Cu···Cu distance in the mixed ligand Cl and PhC_2 complex (2.820(3) Å) is much shorter than that found in a dicapped chloro complex (3.210(4) Å). In fact the shortest distances in trimeric cores are observed when both the capping ligands are acetylide. The short Cu···Cu separation could be attributed to short Cu−C distances. However, an additional electronic influence of the virtual orbitals on HC_2^- cannot be ignored since similar short Cu−O distances do not result in short Cu−Cu distances in hydroxo or phenoxo capped complexes.

The analogous Ag(I) complexes too exhibit similar trends. The complex $Ag_3(dppm)_3(\mu_3\text{-}Cl)_2^+$ has an average Ag···Ag distance of 3.378(2) Å,[40] which is significantly greater than the average Ag···Ag distance in $Ag_3(dppm)_3(\mu_3\text{-}Br)_2^+$ (3.305(3) Å).[41] The acetylide-capped complex $Ag_3(dppm)_3(\mu_3\text{-}C_2Ph)_2^+$ has the shortest Ag···Ag distance (2.944(1) Å).[42] Obviously, a simple geometric model is not sufficient to explain the observed variation of metal−metal distances. These trends appear to be the result of well-defined electronic effects. To understand the electronic factors involved, we have computed the optimized geometry of model trimeric copper complexes using ab initio electronic structure calculations.

The optimized Cu···Cu and Cu−X/Y distances along with the selected natural bond orbital (NBO)[27] analyses data for the models studied have been tabulated in Table 7. The computed Cu···Cu distances are much shorter than that experimentally observed for $Cu_3(dppm)_3(X)(Y)^+$ complexes. The consistently

(40) Franzoni, D.; Pelizzi, G.; Predieri, G.; Tarasconi, P.; Vitali, F.; Pelizzi, C. *J. Chem. Soc., Dalton Trans.* **1989**, 247.
(41) (a) Schubert, U.; Neugebauer, D.; Aly, A. A. M. *Z. Anorg. Allg. Chem.* **1980**, *464*, 217. (b) Aly, A. A. M.; Neugebauer, D.; Orama, O.; Schubert, U.; Schmidbaur, H. *Angew. Chem., Int. Ed. Engl.* **1978**, *17*, 125.
(42) Wang, C.-F.; Peng, S.-M.; Chan, C.-K.; Che, C.-M. *Polyhedron* **1996**, *15*, 1853.

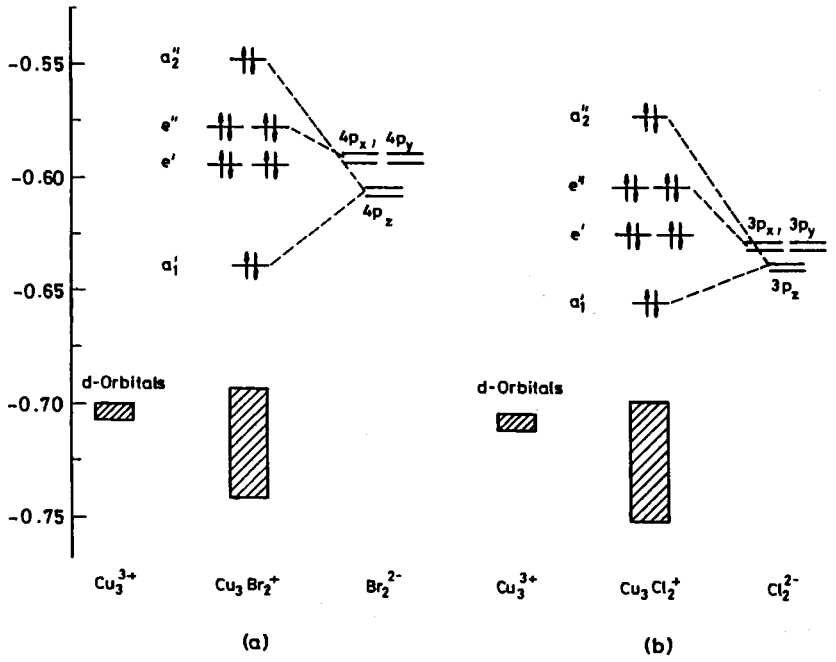

Figure 5. Comparative MO energy level diagram of the filled orbitals of (a) $Cu_3Br_2^+$ and (b) $Cu_3Cl_2^+$. The 15 d orbitals are closely spaced and appear together.

greater Cu···Cu distances observed in the experimental systems could be due to the presence of the dppm ligand, which influences the Cu···Cu distances, in addition to the capping ligands. Although the actual distances do not match, the trends in the optimized Cu···Cu distances reproduce the experimental trends in a remarkable way. The chloro and acetylide caps lead to longer and shorter Cu···Cu distances, respectively. Although the Cu−Br distance is higher in $Cu_3Br_2^+$ than the Cu−Cl in $Cu_3Cl_2^+$, the Cu···Cu distance is shorter in the former. Interestingly none of the monocapped structures could be optimized. Lengthening of the Cu···Cu distances were noted during the process of optimization before failure to find a minimum energy structure. This suggests that the additional restriction of a bridging dppm ligand is necessary to construct a trimeric core if only one cap is present.

Analysis of the energy ordering of the frontier orbitals in the Br and Cl complexes suggests an explanation for the anomalous variation in the Cu···Cu distances mentioned earlier. The frontier occupied orbitals in both $Cu_3Cl_2^+$ and $Cu_3Br_2^+$ complexes have the same symmetry and similar parentage. They are primarily the valence p orbitals on the capping ligands which have mixed with filled d orbitals on the copper cluster (Cu_3^{3+}) having a_2'' and e″ symmetry in an antibonding fashion and the 4p orbitals on the Cu_3^{3+} in a bonding fashion (Figure 5). The HOMO (a_2'') in these two complexes has significant antibonding character between the capping ligands and the Cu_3^{3+} core. This orbital is destabilized to a greater degree in the case of $Cu_3Cl_2^+$ than in $Cu_3Br_2^+$. Similarly, the destabilizing antibonding interaction between the Cu_3^{3+} and the filled p_x and p_y orbitals of the cap having e″ symmetry is less in the case of the Br complex. The orbital having a_1' symmetry, which leads to significant bonding between the cap and the Cu_3^{3+} core, is stabilized to a greater extent in the Br complex. This molecular orbital results from interactions between the p_z orbitals on the cap and the empty 4s orbitals on copper atoms. The stronger interaction of the 4s orbitals on copper atoms leads to a greater stabilization of a_1' in $Cu_3Br_2^+$ than in $Cu_3Cl_2^+$. The higher occupancies computed for the 4s orbitals of copper atoms in $Cu_3Br_2^+$ and the larger Wiberg bond index (WBI)[43] computed for Cu−Br than Cu−Cl confirm this fact. The participation of the vacant 4s orbitals on copper atoms helps in reducing the filled−filled repulsions in the Cu_3^{3+} core and hence decreases the Cu···Cu distance. This effect is much higher when Br rather than Cl is the cap.

The short Cu−C distances alone may not be responsible for the observed Cu···Cu separation in acetylide-capped complexes, and evidence for the electronic effects of the cap becomes apparent from the NBO analysis data. The interaction of the virtual orbitals of the acetylide of suitable symmetry with the d orbitals of Cu_3^{3+} reduces the antibonding nature of the copper cluster core orbitals. The presence of such virtual orbitals in other π-acid capped complexes results in shorter metal−metal distances.[44] The back-donation of electron density from the copper core orbitals to the virtual orbitals is given by the occupancies of the π^* orbitals (0.014×2 in $Cu_3(HC_2)^{2+}$ and 0.017 in $Cu_3Cl(HC_2)^+$) of acetylide. Increase in Cu−C bonding is also noted in the Cu−C WBI values in acetylide-capped complexes. A suitable comparison is provided by the hydroxo-capped species. Although O and C have similar sizes, the Cu−C WBI is significantly higher in $Cu_3(HC_2)_2^+$ than the corresponding Cu−O WBI in the $Cu_3(OH)_2^+$ species (Table 7). The donation of electron density from HC_2^- to the vacant 4s orbitals of copper and the back-donation from the copper d core to the π^* orbital of HC_2^- decrease the Cu···Cu repulsion and increase the Cu−C bonding as well.

The following generalizations can be made based on the above observations. A ligand having filled π orbitals such as Cl^- increases the antibonding nature of the copper core d orbitals and leads to larger Cu···Cu distances. In the case of capping ligands which are larger such as Br^- or I^-, the attenuation of Cu−Cu repulsions from the filled π orbital on the cap is less due to the higher energy and larger size of these orbitals. The large size leads to better overlap with the larger 4s and 4p orbitals on Cu. This leads to better Cu−X bonding. At the same

(43) Wiberg, K. *Tetrahedron* **1968**, *B24*, 1083.
(44) (a) Ratliff, K. S.; Fanwick, P. E.; Kubiak, C. P. *Polyhedron* **1990**, *9*, 1487. (b) Ferguson, G.; Lloyed, B. R.; Puddephatt, R. J. *Organometallics* **1986**, *5*, 344. Also see refs 2c,f,h,l,o.

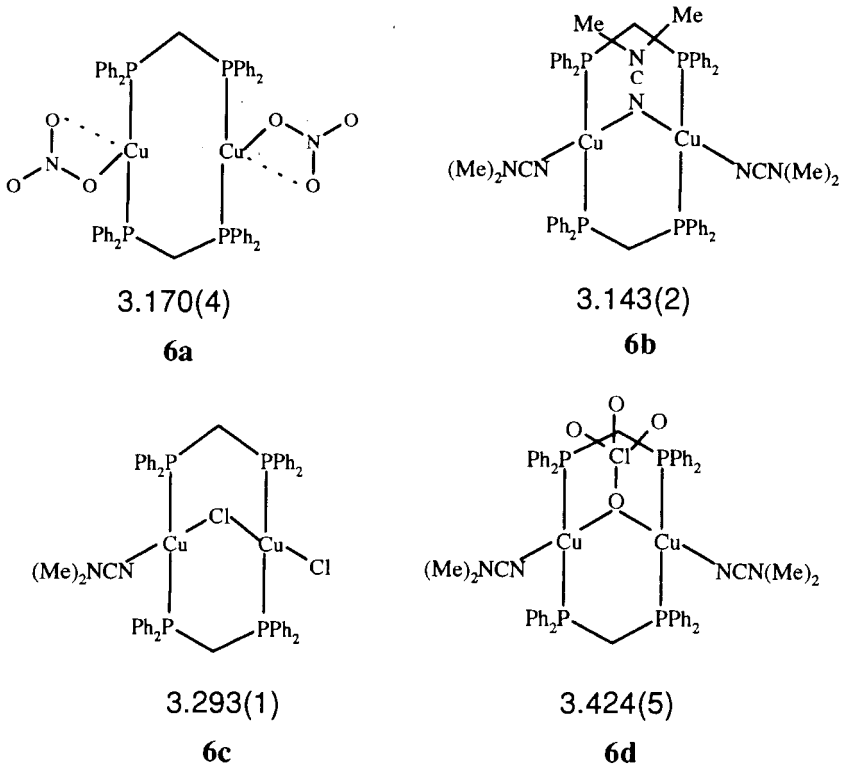

Figure 6. Schematic representation of the structurally characterized dimeric $Cu_2(dppm)_2(\eta^1\text{-}ONO_2)_2$ (**6a**), $Cu_2(dppm)_2(\mu_2\text{-}dmcn)(dmcn)_2(BF_4)_2$ (**6b**), $Cu_2(dppm)_2(dmcn)(\mu_2\text{-}Cl)(Cl)$ (**6c**), and $Cu_2(dppm)_2(dmcn)_2(\mu_2\text{-}OClO_3)(ClO_4)$ (**6d**). The corresponding Cu···Cu distances are also given. Values are taken from ref 15 (**6a**, **6b**, and **6d**) and this work (**6c**).

time, shorter Cu···Cu distances result due to the reduced nature of repulsive interactions. Capping ligands having π-acid character reduce the antibonding nature of the filled d manifold on the copper core through back-donation. This also shortens Cu···Cu distances.

It is gratifying to note that the arguments used to explain the distance variations in $Cu_3(dppm)_3$ complexes can be used to explain variations in the $Cu_2(dppm)_2$ systems also. A schematic diagram of the dimeric complexes and the corresponding Cu···Cu distances are shown in Figure 6. In general, Cu···Cu separations in dimeric complexes are significantly longer than in the trimeric complexes. A three-coordinated $Cu_2(dppm)_2$ complex has a Cu···Cu distance of 3.170(4) Å (**6a**). Introduction of a bridging ligand modulates the Cu···Cu distance. The presence of a weak π acceptor, dmcn as a bridging ligand (**6b**), reduces the Cu···Cu distance marginally. The π donor ligand Cl^- increases the Cu···Cu distance. The Cu···Cu distance in the Cl-bridged complex (**6c**) is significantly longer (0.150 Å) than the dmcn-bridged complex **6b**. Interestingly, the Cu···Cu separation in the ClO_4^--bridged complex (**6d**) is longer than that in the Cl^--bridged complex, where the Cu−Cl−Cu angle is acute and indicative of a 3c-2e bridge.

Solid-State Luminescence Spectra and Nuclearity. The nuclearity of Cu(I)−dppm complexes could be identified based on their solid-state luminescence spectra. All trinuclear complexes show a common broad band centered around 510−520 nm (Table 5). A similar band observed by Harvey et al. in $Cu_3(dppm)_3(OH)(BF_4)_2$ has been assigned to a state that is different "from a localized independent excited CuP_2^+ center but rather is delocalized within the Cu_3 frame".[45] Similarly, the luminescence bands of $Cu_4X_4L_4$ clusters (X are halide ions and L are nitrogen donor ligands) have been assigned to a transition involving copper-centered excited state strongly modified by Cu···Cu interactions.[46] As the Cu···Cu distances in trimeric complexes are generally shorter than in the dimers, the presence of such copper cluster centered emissive states[47] is more likely in $Cu_3(dppm)_3$ complexes. Although the Br and I complexes exhibit the high-energy emission bands (484 and 466 nm, respectively), these are not distinct in the Cl and OH complexes, where it is masked by the lower energy band at 511 nm. The emission spectrum of the Cl complex is particularly broad (Figure 4b). Interestingly, the Br and I complexes show extra bands around 566 and 574 nm, respectively. On the other hand, the absence of the low-energy band around 510 nm and the presence of emissions around 465−485 nm characterize the luminescence spectra of the dimeric $Cu_2(dppm)_2$ complexes. The invariance of this band in several $Cu_n(dppm)_n$ complexes has been used to assign this band to an emission originating from an intraligand phosphine excited state.[48] Identification of a trimeric core from the emission spectra is feasible, although confirmation of the assignments mentioned needs further study.

Conclusion

The nuclearity and Cu···Cu distances in copper(I)−dppm complexes are controlled by the bridging ligands present. Ligands such as halides and hydroxide prefer a trinuclear core. In case suitable caps are not present, a dimeric complex is dictated by the dppm ligand. The instability of the hydroxide-

(45) Harvey, P. D.; Provencher, R. *Inorg. Chem.* **1996**, *35*, 2235.
(46) Henary, M.; Zink, J. I. *J. Am. Chem. Soc.* **1989**, *111*, 7407, and references therein.
(47) Barrie, J. D.; Dunn, B.; Hollingsworth, G.; Zink, J. I. *J. Phys. Chem.* **1989**, *93*, 3958.
(48) Li, D.; Che, C.-M.; Wong, W.-T.; Shieh, S.-J.; Peng, S.-M. *J. Chem. Soc., Dalton Trans.* **1993**, 653.

bridged complex in the presence of acid suggests that the organization of a trinuclear core requires two π electron pairs on the donor cap. In solution, however, these complexes are labile and are in equilibrium with dimeric species. One such complex has been trapped by the addition of excess dmcn and structurally characterized. The nuclearity of the species in the solid-state can be determined from the emission spectra of the complexes. Both dppm and the bridging ligand dictate the Cu···Cu distances in these systems. Ab initio electronic structure calculations suggest why these distances vary the way they do. The presence of a good π donor increases the Cu···Cu antibonding interactions, and a good π acceptor reduces the same. Designed synthesis of copper(I)−dppm complexes with predetermined Cu···Cu distances and nuclearity appears feasible.

Acknowledgment. This work was supported by a grant from CSIR (New Delhi).

Note Added in Proof. A relevant reference reporting a structure very similar to 2·THF (core structure $Cu_3(dppm)_3(\mu_3\text{-}Br)_2^+$) has appeared recently: Lang, J.-P.; Tatsumi, K. *Inorg. Chem.* **1998**, *37*, 6308.

Supporting Information Available: Listing of the atomic coordinates and equivalent isotropic displacement parameters, all bond lengths and angles, anisotropic displacement parameters, and hydrogen coordinates and isotropic displacement parameters of complexes **2**, **3**, and **4**. The solid-state emission and the corresponding excitation spectra of the complexes recorded at room temperature are also given (22 pages). Ordering information is given on any current masthead page.

IC980515F